



Calibration of Optical Testing System for Dynamic Impact Experiment of Aviation Seat

Xiang Liu^(✉), Hongyi Gao, Rubing Wang, and Shaoyin Wu

Aerospace Life-Support Industries, Ltd., Xiangyang 441003, China
liux.ali@hotmail.com

Abstract. In this paper, a complete set of optical testing system calibration method combining three-dimensional control field design and space resection calculation program development for dynamic impact experiment of aviation seat have been formed, which can obtain high-precision calibration parameters of high-speed camera: exterior orientation elements, interior orientation elements and optical distortion coefficients, and the effectiveness and accuracy of this method were verified by tests. This research content provides important data support for the subsequent use of intersection method to solve the high-precision three-dimensional trajectory and attitude of the occupant head in the dynamic impact experiment of aviation seat.

Keywords: Calibration · Optical testing system · Aviation seat · Dynamic impact experiment · Space resection

1 Introduction

Aviation seat is an important part of aircraft airborne system, which not only provides a comfortable experience for the occupants, but also plays an important role in safety protection and emergency evacuation of the occupants when the aircraft is in emergency state [1, 2]. In accordance with the requirements of crashworthiness provisions in the airworthiness regulations of CCAR-23-R3 [3], CCAR-25-R4 [4], CCAR-27-R2 [5], CCAR-29-R2 [6], etc., dynamic impact experiment is a part of airworthiness certification process of aviation seat [7, 8]. The necessary link mainly verifies the safety performance of aviation seat for occupant protection during simulated crash and impact process.

In the dynamic impact experiment of aviation seat, the optical testing system usually consists of lateral high-speed camera, top high-speed camera and vehicle-mounted high-speed camera. In addition to recording the experiment process, lateral high-speed camera is also used to calculate two-dimensional or three-dimensional occupant head trajectory and attitude according to the requirements of test task. Calibration of exterior orientation elements, interior orientation elements and optical distortion coefficients of lateral high-speed camera can restore correct shape of each image beam [9, 10], which is an effective guarantee for the solution of high-precision occupant head trajectory and attitude by close-range photogrammetry processing method.

2 Principle of Calibration Model

2.1 Calibration Content of High-Speed Camera

Calibration parameters mainly include three parts: interior orientation elements, exterior orientation elements and optical distortion coefficients [11].

- **Interior orientation elements.** Interior orientation elements of high-speed camera are parameters that describe relative position between photography center and image, including principal distance f and image principal point coordinates (x_0, y_0) .
- **Exterior orientation elements.** Exterior orientation elements are parameters of spatial position and attitude of image photography moment in space coordinate system, which contain six parameters, namely three line elements (X_S, Y_S, Z_S) and three angle elements $(\varphi, \omega, \kappa)$.
- **Optical distortion coefficients.** Due to manufacturing process of high-speed camera lens, actual image point deviates from ideal point, resulting in optical distortion difference [12]. Optical distortion mainly includes radial distortion and tangential distortion. In actual high-precision photogrammetry, nonlinear imaging model considering optical distortion should be used to describe imaging relationship.

2.2 High-Speed Camera Imaging Model

The imaging model of high-speed camera used for optical measurement is usually central projection imaging model, and its mathematical basis is collinearity condition equation [13]. The central projection imaging model considering optical distortion correction is expressed as:

$$\begin{cases} x - x_0 + \Delta x = -f \frac{a_1(X-X_S)+b_1(Y-Y_S)+c_1(Z-Z_S)}{a_3(X-X_S)+b_3(Y-Y_S)+c_3(Z-Z_S)} \\ y - y_0 + \Delta y = -f \frac{a_2(X-X_S)+b_2(Y-Y_S)+c_2(Z-Z_S)}{a_3(X-X_S)+b_3(Y-Y_S)+c_3(Z-Z_S)} \end{cases} \quad (1)$$

In the formula: x, y are measured image coordinates; x_0, y_0, f are interior orientation elements; X_S, Y_S, Z_S are exterior orientation line elements; X, Y, Z are space coordinates; $\Delta x, \Delta y$ are optical distortion correction values of image coordinates; a_i, b_i, c_i ($i = 1, 2, 3$) are 9 direction cosines composed of exterior orientation angle elements.

2.3 Principle of Space Resection

Linearization of Collinearity Condition Equation. Since collinearity condition equation is a nonlinear function, it is necessary to expand collinearity condition equation into

a linear form by Taylor formula [14]. Linearized error equation is obtained as follow:

$$\begin{bmatrix} v_x \\ v_y \end{bmatrix} = \begin{bmatrix} a_{11} & a_{12} & a_{13} & a_{14} & a_{15} & a_{16} \\ a_{21} & a_{22} & a_{23} & a_{24} & a_{25} & a_{26} \end{bmatrix} \begin{bmatrix} \Delta X_s \\ \Delta Y_s \\ \Delta Z_s \\ \Delta \varphi \\ \Delta \omega \\ \Delta \kappa \end{bmatrix} + \begin{bmatrix} a_{17} & a_{18} & a_{19} \\ a_{27} & a_{28} & a_{29} \end{bmatrix} \begin{bmatrix} \Delta f \\ \Delta x_0 \\ \Delta y_0 \end{bmatrix} + \begin{bmatrix} b_{11} & b_{12} & b_{13} & b_{14} \\ b_{21} & b_{22} & b_{23} & b_{24} \end{bmatrix} \begin{bmatrix} \Delta k_1 \\ \Delta k_2 \\ \Delta p_1 \\ \Delta p_2 \end{bmatrix} - \begin{bmatrix} x - (x) \\ y - (y) \end{bmatrix} \tag{2}$$

In the formula: v_x, v_y are correction values of image coordinates; $\Delta X_s, \Delta Y_s, \Delta Z_s, \Delta \varphi, \Delta \omega, \Delta \kappa, \Delta f, \Delta x_0, \Delta y_0, \Delta k_1, \Delta k_2, \Delta p_1, \Delta p_2$ are correction values of calibration parameters; x, y are image coordinate measurement values; $(x), (y)$ are image coordinates calculated by substituting approximate value of unknown into collinearity equation.

Basic Method of Space Resection. In order to improve the solution accuracy, redundant equations are usually required, so the least squares adjustment method should be used for calculation [15]. Considering that observed values of all image coordinates are generally regarded as equal-precision measurements, the expression of normal equation solution is obtained as follow:

$$X = (A^T A)^{-1} A^T L \tag{3}$$

Thereby, correction values of approximate quantities of calibration parameters are obtained. In each iteration, the sum of unknown approximate quantity and correction value calculated in the previous iteration is used as a new approximation value, and calculation process is repeated until the correction value is less than a certain limit. Finally, solutions of 13 parameters are obtained.

The above is basic method of space resection, and the implementation of subsequent calibration scheme is carried out according to this method. Space resection solution based on collinearity condition equation is an analytical photogrammetry calibration method of test field for optical testing system. This method is easy to implement in test field and has high universality.

3 Technical Scheme of High-Speed Camera Calibration

3.1 Technical Route of High-Speed Camera Calibration

Technical route of high-speed camera calibration is mainly divided into two parts: on-site operation in control field and indoor data processing. Technical route diagram is shown in Fig. 1.

On-site operation in control field mainly focuses on the layout of three-dimensional control field and erection of high-speed camera. The operation process starts with the

design and construction of three-dimensional control field and the reasonable arrangement of a certain number of mark points; then mark points space coordinates are measured by the total station; and finally, the images of mark points are recorded by high-speed camera.

Indoor data processing mainly relies on the interpretation software and self-written resection calculation program to calculate space coordinates and image coordinates of previous recorded mark points. The processing flow is as follows: firstly, the image coordinates of mark points are interpreted by interpretation software; then, the calibration parameters are obtained by using self-written space resection calculation program to process relevant data; and finally, the calibration parameters and image coordinates of verification points are substituted into intersection calculation program to calculate space coordinates of verification points.

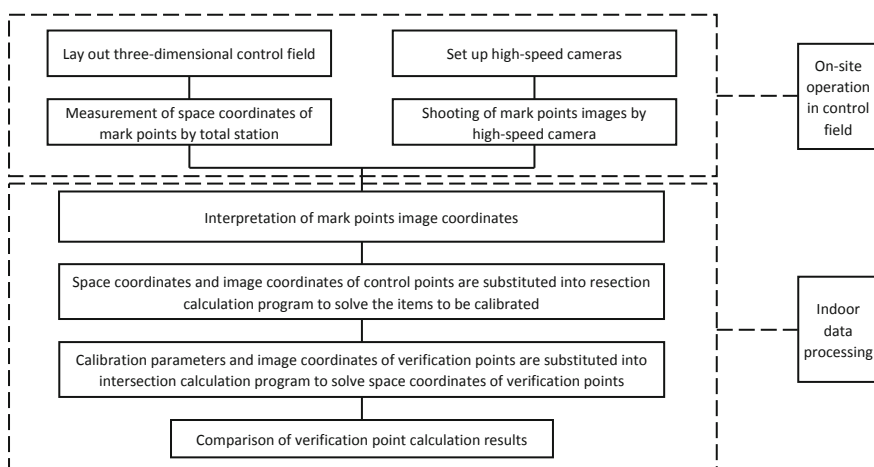


Fig. 1. Technical route of high-speed camera calibration

3.2 Three-Dimensional Control Field Design

In view of dynamic impact test scene of aviation seat, this calibration scheme arranges three-dimensional control field in the dynamic impact test platform, and the placement state of optical testing system is consistent with the specific test layout during the test. The design can ensure the accurate connection between the calibration of optical testing system and the measurement of dynamic targets.

Establishment of three-dimensional Control Field Coordinate System. In the dynamic impact experiment of aviation seat, absolute spatial orientation of target is not needed to be considered in measurement of three-dimensional position and attitude. Therefore, the space coordinate system of three-dimensional control field adopts a customized independent coordinate system according to a certain setting principle.

The setting diagram of the three-dimensional control field coordinate system is shown in Fig. 2. Three-dimensional control field adopts right-hand coordinate system, with

the horizontal position of the vertical axis of total station as the plane origin, and the intersection of vertical and horizontal axes of total station as the elevation origin. Heading direction of dynamic impact test platform is selected as X-axis of the coordinate system, Y-axis is perpendicular to the X-axis and in the vertical plane, Z-axis is perpendicular to the X-axis and in the horizontal plane.

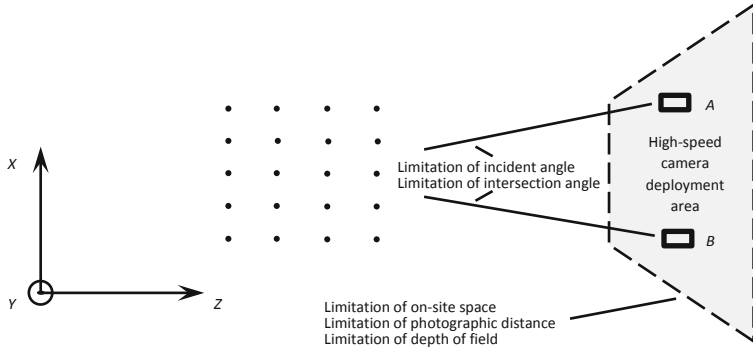


Fig. 2. Schematic diagram of layout position of three-dimensional control field

Selection of Mark Point. This calibration scheme adopts dual-color cross mark. In the scheme, TEMA motion image analysis software is used to interpret marks of control point and verification point in the high-speed images, and it sets up corresponding automatic image recognition and tracking mode for dual-color cross mark points. recognition accuracy of this mode is able to reach 1/3 pixel. meanwhile, in order to verify the accuracy of attitude calculation, a set of target plates is also designed in this calibration scheme (see Fig. 3). Centers of three mark points are distributed on target plate, which are ranked as 1, 2 and 3, and line 1–2 is perpendicular to line 2–3.

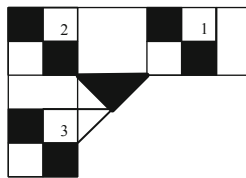


Fig. 3. Design of target plate

Technical Conditions for Establishment of Three-Dimensional Control Field.

The quantity, quality and distribution of mark points directly affect the calibration accuracy [16]. Therefore, establishment of three-dimensional control field should meet the following technical conditions:

- A sufficient number of mark points should be laid out.
- Mark points are evenly distributed in the three coordinate directions and have sufficient extension.

- Coordinate measurement of mark point should be stable and reliable to improve measurement accuracy.
- Artificial light source is used for illumination in control field, which can improve light intensity to make image clear.
- Intersection angle of each mark point is preferably $60^\circ \sim 120^\circ$.
- Photographic incident angle of each mark point is preferably less than 45° .
- Motion range of dynamic target should be roughly the same as photograph distance.

In conclusion, the calibration scheme should uniform distribution of mark points, as well as maximizing the measurement accuracy of control point coordinates, so as to ensure high precision and high reliability of the calibration. Based on the above constraints, the layout diagram of three-dimensional control field is shown in Fig. 2.

3.3 Space Resection Calculation Program Development

This calibration scheme uses Python language to write space resection calculation program, which can be used to input space coordinates of control points and coordinates of image points to calculate corresponding high-speed camera calibration parameters.

Algorithm of Space Resection Calculation Program. Combined with theoretical derivation of high-speed camera imaging model, the overall solution process of this algorithm is as follows:

1. Obtain the known data: Obtain image coordinates of the control point x_i, y_i from the image data; and obtain space coordinates of the control point X_i, Y_i, Z_i from three-dimensional control field observation results.
2. Determine the initial value of the unknowns: Since coordinates of principal point x_0, y_0 and optical distortion coefficients k_1, k_2, p_1 and p_2 are small values, these initial value are set to 0; the initial value of principal distance f is set to nominal focal length of lens; the initial values of exterior orientation line elements $X_S, Y_S,$ and Z_S are measurement results of total station to estimated photographic center; the initial values of exterior orientation angle elements $\varphi, \omega,$ and κ are measurement values of protractor.
3. Calculate the rotation matrix \mathbf{R} : Calculate the direction cosine value by using the approximate value of exterior orientation elements and form matrix \mathbf{R} .
4. Calculate the approximate value of image coordinate: Calculate the approximate value of image coordinate of the control point $(x), (y)$ according to collinearity condition equation.
5. Compose the error equation: Calculate the coefficients and constant terms of the error equation point by point.
6. Compose the normal equation: Calculate the coefficient matrix $\mathbf{A}^T\mathbf{A}$ and constant terms of the normal equation $\mathbf{A}^T\mathbf{L}$.
7. Solve the calibration parameters: According to the normal equation, solve the correction value of exterior orientation elements, interior orientation elements and optical distortion coefficients, and sum up with the corresponding approximate values to obtain new the approximate value of each calibration parameter.

8. Check the convergence of the calculation: Compare the correction value of each calibration parameter with the specified tolerance. If the correction value is less than the tolerance, the calculation is terminated; otherwise, repeat the calculation steps 3 to 7 with new approximation value until the requirements are met.

File for Space Resection Calculation Program. The input and output file format of space resection calculation program is CSV file format. During data processing, first convert image coordinates interpreted by Tema software into standard CSV format, and record space coordinates into CSV file. Space resection calculation program imports CSV file and reads image coordinates and space coordinates of each point in turn, and finally generates CSV file with calibration parameters. Calibration parameter file can be used as basic file for subsequent intersection calculation, and can also be directly called to participate in subsequent space coordinate calculation. Flow diagram of space resection calculation program file is shown in Fig. 4.

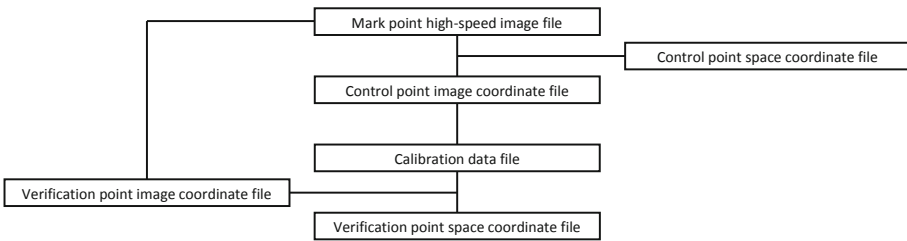


Fig. 4. Program file flow diagram

4 Test Validation and Analysis

4.1 Design of Verification Test Scheme

Considering requirements of dynamic impact experiment of aviation seat and the application scenario of optical testing system, the verification test was carried out on dynamic impact platform. According to layout principle and technical requirement of the three-dimensional control field, high-speed cameras on both sides were erected symmetrically with the center line of three-dimensional control field. The distance from center plane of three-dimensional control field was about 6.2 m, and the intersection angle was about 30°. In order to adapt to the automatic identification and tracking of image point coordinates, the imaging size of mark point should be 20 pixels, and the size of mark was finally determined to be 5 cm. Based on the requirement of redundant observation, a total of 13 control points and 14 verification points were arranged in this verification test. The high-speed camera used in the test was Photron BC2-HD, with resolution of 2048 × 1536 pixels and individual pixel size of 10 μm. The nominal focal length of lens was 35 mm.

In this verification test, a total of 5 sets of verification point images were taken, including 4 sets of images of different placement states of the target plate and 1 set of

benchmark length verification point images. The target plate was set up in 4 placement states: no yaw-no pitch-roll, no yaw-pitch-roll, yaw-no pitch-roll, yaw-pitch-roll, which basically covered the actual situation.

After loading the images into TEMA software, the dual-color mark tracking mode was selected to automatically identify and measure mark points. The measured image point coordinates were exported in tabular form. The previous data files were substituted into the space resection calculation program and space intersection calculation program to obtain calibration parameters of high-speed cameras and space coordinates of verification points.

4.2 Verification and Analysis of Calibration Results

After calculating space coordinates and image coordinates of the 13 control points, the calibration parameters of high-speed cameras on both sides were obtained, as shown in Table 1. This verification scheme was mainly compared and verified from three aspects: space coordinates, structural angle, size and length. In the comparison and verification, since the measurement accuracy of total station was higher than that of photogrammetry method, the measurement result of total station was regarded as true value and used as reference value for comparison.

Table 1. Calibration parameters of high-speed camera (unit: mm)

Calibration parameters	Right-side high-speed camera	Left-side high-speed camera
X_s	5821.99365	2793.34057
Y_s	-351.63909	-363.83842
Z_s	-33.56439	-72.68824
φ	-0.30104	0.23281
ω	-0.07185	-0.06741
κ	0.01000	0.00742
f	34.81280	34.11824
x_0	0.05435	-0.25367
y_0	-0.38352	0.17955
k_1	8.8737823203e-05	1.7251928477e-04
k_2	-3.7038371663e-07	-9.9204570813e-07
p_1	7.7781131501e-06	1.2798750490e-04
p_2	-8.4795365993e-06	-7.0196636780e-05

Verification of Space Coordinates. Table 2 lists space coordinate values of the 12 verification points in X , Y , and Z directions of four groups of target plates in different placement states. By comparing with the measurement data of total station, the maximum difference is -1.78 mm and minimum difference is -0.10 mm in X direction, the

maximum difference is 0.80 mm and minimum difference is 0.01 mm in Y direction, and the maximum difference is -1.92 mm and minimum difference is -0.13 mm in Z direction. The root mean square error in each direction RMS_X is 1.20 mm, RMS_Y is 0.51 mm, and RMS_Z is 1.02 mm. According to the comparison data, the space coordinates calculated by the calibration parameters of high-speed camera are able to reach an accuracy better than ± 2 mm, and this accuracy range can meet the test accuracy requirements of current routine experiments.

Table 2. Comparison of space coordinates (unit: mm)

Number	$X_{measure}$	$Y_{measure}$	$Z_{measure}$	X_{true}	Y_{true}	Z_{true}	ΔX	ΔY	ΔZ
T1-1	2771.81	-804.59	-5630.37	2772.90	-804.60	-5629.70	-1.09	0.01	-0.67
T1-2	2674.50	-805.22	-5627.75	2674.60	-805.50	-5626.70	-0.10	0.28	-1.05
T1-3	2675.44	-868.09	-5591.54	2676.80	-868.60	-5592.80	-1.36	0.51	1.26
T2-1	2771.11	-1034.20	-5496.23	2772.10	-1034.50	-5496.10	-0.99	0.30	-0.13
T2-2	2703.80	-972.94	-5531.01	2704.70	-973.40	-5531.60	-0.90	0.46	0.59
T2-3	2651.32	-1016.26	-5504.96	2652.20	-1016.80	-5506.50	-0.88	0.54	1.54
T3-1	2805.53	-804.47	-5709.62	2806.20	-804.70	-5707.70	-0.67	0.23	-1.92
T3-2	2711.62	-805.38	-5682.58	2712.50	-805.90	-5682.30	-0.88	0.52	-0.28
T3-3	2721.82	-868.12	-5647.85	2723.60	-868.90	-5648.70	-1.78	0.78	0.85
T4-1	2839.12	-1034.10	-5579.95	2840.70	-1034.70	-5580.60	-1.58	0.60	0.65
T4-2	2764.76	-972.95	-5596.37	2766.10	-973.50	-5596.10	-1.34	0.55	-0.27
T4-3	2720.48	-1016.20	-5557.95	2722.20	-1017.00	-5559.20	-1.72	0.80	1.25
RMS							1.20	0.51	1.02

Verification of Structural Angle. The verification of structural angle requires the use of target plate, and the structural angle is three inner angles of the triangle connecting the center of target plate mark point. Table 3 lists three structural angles of four groups of target plates in different placement states. By comparing with theoretical calculated values, the maximum and minimum differences of $\angle 123$ are 0.35° and 0.14° , the maximum and minimum differences of $\angle 213$ are -0.22° and 0.02° , and the maximum and minimum differences of $\angle 132$ are -0.26° and 0.01° ; the root mean square error of each inner angle $RMS_{\angle 123}$ is 0.26° , $RMS_{\angle 213}$ is 0.16° , and $RMS_{\angle 132}$ is 0.16° ; standard deviation of inner angle $\sigma_{\angle 123}$ is 0.25° , $\sigma_{\angle 213}$ is 0.18° , $\sigma_{\angle 132}$ is 0.11° . The structural angle of target plate calculated by calibration parameters of high-speed camera can achieve an accuracy better than $\pm 0.4^\circ$, and standard deviation of structural angle is within 0.3° . The above shows that the measurement data is consistent.

Verification of Size and Length. The comparison and verification of target plate size and length mainly examines the relative position accuracy, which to a certain extent avoids systematic error compared with true value of absolute space coordinate in object space coordinate system. Size of target plate is defined as the length of three sides of line connecting target plate mark point center. The size of target plate and distance between verification points are measured with a tape measure as true value of length. Table 4 lists four groups of target plate sizes in different placement states, and Table 5 lists

Table 3. Comparison of structural angle (unit:°)

Number	$\angle 123_{\text{measure}}$	$\angle 213_{\text{measure}}$	$\angle 132_{\text{measure}}$	$\angle 123_{\text{true}}$	$\angle 213_{\text{true}}$	$\angle 132_{\text{true}}$	$\Delta\angle 123$	$\Delta\angle 213$	$\Delta\angle 132$
T1	90.35	36.57	53.08	90.00	36.66	53.34	0.35	-0.09	-0.26
T2	89.79	36.87	53.35	90.00	36.66	53.34	-0.21	0.21	0.01
T3	90.30	36.44	53.26	90.00	36.66	53.34	0.30	-0.22	-0.08
T4	90.14	36.68	53.19	90.00	36.66	53.34	0.14	0.02	-0.15
σ	0.25	0.18	0.11			RMS	0.26	0.16	0.16

separation distance of the benchmark verification points. By comparing with the tape measured value, the maximum difference and minimum difference of L_{13} are 0.57 mm and 0.02 mm, the maximum difference and minimum difference of L_{12} are 0.33 mm and 0.03 mm, the maximum difference and minimum difference of L_{23} are 0.36 mm and 0.06 mm; the root mean square error of each side length $RMS_{L_{13}}$ is 0.43 mm, $RMS_{L_{12}}$ is 0.22 mm, and $RMS_{L_{23}}$ is 0.26 mm; The standard deviation of the same side length in different states $\sigma_{L_{13}}$ is 0.25 mm, $\sigma_{L_{12}}$ is 0.18 mm, and $\sigma_{L_{23}}$ is 0.22 mm; the difference of reference length L_{S1-S2} is 1.86 mm, and the relative error is 0.09%. The length of line connecting center of target plate mark points calculated by high-speed camera calibration parameters can achieve an accuracy better than ± 0.5 mm. The standard deviation of target plate size in different placement states is within 0.3 mm, and the relative accuracy of reference length is within 1/1000. The above reflects the high accuracy of relative positional relationship of object points in the digital photogrammetry results based on calibration parameters.

Table 4. Comparison of target plate size (unit: mm)

Number	$L_{13\text{measure}}$	$L_{12\text{measure}}$	$L_{23\text{measure}}$	$L_{13\text{true}}$	$L_{12\text{true}}$	$L_{23\text{true}}$	ΔL_{13}	ΔL_{12}	ΔL_{23}
T1	121.77	97.35	72.56	121.42	97.40	72.50	0.35	-0.05	0.06
T2	121.44	97.43	72.86	121.42	97.40	72.50	0.02	0.03	0.36
T3	121.95	97.73	72.43	121.42	97.40	72.50	0.53	0.33	-0.07
T4	121.99	97.67	72.86	121.42	97.40	72.50	0.57	0.27	0.36
σ	0.25	0.18	0.22			RMS	0.43	0.22	0.26

Table 5. Comparison of reference length (unit: mm)

Number	X_{measure}	Y_{measure}	Z_{measure}	$L_{S1-S2\text{measure}}$	$L_{S1-S2\text{true}}$	ΔL_{S1-S2}
S_1	3150.60	-192.05	-5518.37	2098.36	2096.50	1.86
S_2	5248.96	-191.43	-5519.17			

5 Conclusion

The main research content of this paper is the calibration of exterior orientation elements, interior orientation elements and optical distortion coefficients of high-speed camera in the dynamic impact experiment of aviation seat based on the space resection principle. Firstly, starting from the fact that collinearity condition is mathematical basis of central projection imaging, high-speed camera imaging model is constructed, and space resection relation is deduced. Next, according to the principle of space resection, the operation process of high-speed camera calibration is determined. Three-dimensional control field is laid out, and space resection calculation program is written to realize calibration of high-speed camera. Finally, intersection calculation results obtained based on calibration parameters are compared and analyzed with measurement data of total station to verify effectiveness and accuracy of this method. The research on calibration of optical testing system for dynamic impact experiment of aviation seat provides data basis for the subsequent three-dimensional trajectory and attitude calculation of the occupant head.

References

1. Li, M.X., Xiang, J.W., Ren, Y.R., et al.: Crashworthiness evaluation and analysis method of aircraft seat. *J. Beijing Univ. Aeronaut. Astronaut.* **42**(2), 383–390 (2016)
2. Feng, Z.Y., Yang, Y.P., He, Y.L., et al.: Research on vertical dynamic characteristics of aviation dummy under seat constraint. *Eng. Mech.* **37**(08), 246–256 (2020)
3. Civil Aviation Administration of China: CCAR-23-R3 Airworthiness standards of normal, utility, acrobatic, and commuter category airplanes. Civil Aviation Administration of China, Beijing (2005)
4. Civil Aviation Administration of China: CCAR-25-R4 Airworthiness standard of transport aircraft. Civil Aviation Administration of China, Beijing (2011)
5. Civil Aviation Administration of China: CCAR-27-R2 Airworthiness standards of normal category rotorcraft. Civil Aviation Administration of China, Beijing (2017)
6. Civil Aviation Administration of China: CCAR-29-R2 Airworthiness standards of transport category rotorcraft. Civil Aviation Administration of China, Beijing (2017)
7. Wang, Y.F., Miao, J., Zhang, J.T.: Research on dynamic airworthiness test technology of aviation seat. *Equip. Manuf. Technol.* **2020**(6), 236–239 (2020)
8. Wang, X.Z., Dong, D., Li, F., et al.: Relationship between the HIC and the head path of the dummy in civil aircraft seats during the 16g dynamic test. *Modern Mach.* **2020**(02), 47–51 (2020)
9. Luhmann, T., Fraser, C., Maas, H.G.: Sensor modelling and camera calibration for close-range photogrammetry. *ISPRS J. Photogramm. Remote Sens.* **115**(05), 37–46 (2016)
10. Liu, Z., Wu, Q., Wu, S., et al.: Flexible and accurate camera calibration using grid spherical images. *Optics Express* **25**(13), 15269 (2017)
11. Li, A.: Research on Calibration Technology of Non-metric Digital Camera. Shandong University of Science and Technology, Qingdao (2019)
12. Yang, B.W., Guo, X.S.: Overview of nonlinear distortion correction of camera lens. *J. Image Graph.* **10**(3), 269–274 (2012)
13. Abdel-Aziz, Y.I., Karara, H.M.: Direct linear transformation from comparator coordinates into object space coordinates in close-range photogrammetry. *Photogramm. Eng. Remote Sens.: J. Am. Soc. Photogramm.* **81**(2), 103–107 (2015)

14. Wang, L.H., Li, L.L., Guo, H.L.: A target-based calibration method. *Beijing Surv. Map.* **35**(3), 372–375 (2021)
15. Yao, N., Lin, Z.R., Ren, C.F., et al.: A distortion model suitable for nonlinear distortion correction of digital video camera. *Laser Optoelectr. Progr.* **51**(2), 171–178 (2014)
16. Wu, S.Y.: *Research on Optical Sensor Geometric Calibration Technology*. JiMei University, Xiamen (2013)